



Original article

Design, synthesis and biological evaluation of novel (E)- α -benzylsulfonyl chalcone derivatives as potential BRAF inhibitors

Qing-Shan Li, Cui-Yun Li, Xiang Lu, Hui Zhang, Hai-Liang Zhu*

State Key Laboratory of Pharmaceutical Biotechnology, Nanjing University, Nanjing 210093, PR China

ARTICLE INFO

Article history:

Received 17 September 2011

Received in revised form

2 February 2012

Accepted 3 February 2012

Available online 11 February 2012

Keywords:

BRAF

Mutant

Inhibitors

Melanoma

Virtual screening

ABSTRACT

Activating mutations in the BRAF serine/threonine kinase are found in more than 70% of human melanomas, >90% of which are BRAF^{V600E}. It provides new therapeutic opportunities in malignant melanoma. *In silico* and *in vitro* screening of our compound collection has identified **Hit 2** as BRAF^{V600E} inhibitor. Based on its structure, a series of novel (E)- α -benzylsulfonyl chalcone derivatives (**13–40**) were designed and synthesized. Compound **38** exhibited the most potent inhibitory activity with an IC₅₀ value of 0.17 μ M for BRAF^{V600E} and GI₅₀ value of 0.52 μ M for mutant BRAF-dependent cells. The results of cell based pERK activity and cellular selectivity suggested that those compounds could selectively inhibit proliferation of mutant BRAF-dependent melanoma cell line through inhibition of oncogenic BRAF.

© 2012 Elsevier Masson SAS. All rights reserved.

1. Introduction

The mitogen-activated protein kinase (MAPK) signal transduction pathway regulates cellular growth, proliferation, and differentiation in response to many different external stimuli [1,2]. MAP kinases are regulated by phosphorylation cascades whereby activation of an upstream kinase leads to phosphorylation of a downstream substrate which itself has protein kinase activity [3,4]. V-RAF murine sarcoma viral oncogene homolog B1 (termed as BRAF) [5] is a serine/threonine specific protein kinase that has long been viewed as key players in the MAPK pathway [6,7]. Under normal circumstances, BRAF is activated downstream of receptors in the cell membrane in a RAS small G-protein dependent manner. It then phosphorylates and activates the protein kinase MEK and ERK orderly, regulating gene expression and controlling how cells respond to extracellular signals [6,8].

Cancers arise owing to the accumulation of mutations in critical genes that alter normal programmes of cell proliferation, differentiation and death [9]. Clinically, BRAF has a high rate of activating mutation in a number of cancers, such as melanoma, papillary

thyroid, colorectal, and ovarian [10–12]. Melanomas in particular show a high incidence of BRAF mutations, the most common being a substitution of glutamic acid for valine at position 600 (V600E). This substitution, which lies within the kinase activation loop, essentially precludes the need for phosphorylation and results in constitutively active BRAF that displays approximately a 500-fold increase in kinase activity over the wild-type isoform [13–15]. Oncogenic BRAF^{V600E} bypasses the requirement for upstream regulation by phosphorylation that results in a MAPK signaling pathway that is constitutively activated in the absence of extracellular growth factor signals, inducing uncontrolled cell proliferation, increased cell survival, and tumor progression. Inhibition of mutant BRAF signaling, through either direct inhibition of the enzyme or inhibition of MEK, has been demonstrated preclinically to inhibit tumor growth [16–18]. Very recently, treatment of BRAF mutant melanoma patients with a selective BRAF inhibitor has resulted in antitumor activity [19,20], validating mutant BRAF as a therapeutic target and offering opportunities for anti-melanoma drug development.

The interest in developing new drugs targeting the MAP kinase pathway has increased considerably, and inhibitors are currently being tested in preclinical and clinical trials [17]. The most intensely studied, sorafenib, was used in the treatment of advanced renal cancer, proved to be active against BRAF in cellular assays [21]. Several BRAF inhibitors that were identified through solution screening have been described in the literature [22,23]. The availability of the crystal structure of the BRAF protein kinase [23] now

Abbreviations: BRAFhomolog B1, V-RAF murine sarcoma viral oncogene; pERK, phosphorylated extracellular regulated kinase; BRAF^{V600E}, V600E mutant BRAF; BRAF^{WT}, BRAF wild-type; IC₅₀, half maximal inhibitory concentration; GI₅₀, the concentration that causes 50% growth inhibition.

* Corresponding author. Tel./ fax: +86 25 83592672.

E-mail address: zhuhl@nju.edu.cn (H.-L. Zhu).

provides an opportunity for utilizing the virtual screening strategy to identify oncogenic BRAF inhibitors from our compound collection. Based on calculated binding abilities with BRAF structure which generated from the *in silico* screening, five hits (Table 1) were selected for initial protein kinase inhibitory activities screening. Among them (E)-2-(Benzylsulfonyl)-3-(4-fluorophenyl)-1-phenylprop-2-en-1-one (**Hit 2**) exhibited the best BRAF^{V600E} inhibitory ability, with IC₅₀ value of 1.04 μ M. In order to obtain more potent BRAF^{V600E} inhibitors, various substitutions were introduced to the aromatic systems of (E)- α -benzylsulfonyl chalcone skeleton. Then twenty-eight (E)- α -benzylsulfonyl chalcone derivatives were synthesized and evaluated as oncogenic BRAF^{V600E} inhibitors, their antiproliferative activities against BRAF mutant melanoma cells were also measured. Some compounds exhibited favorable activities deserve further research as therapeutic of BRAF mutant melanoma.

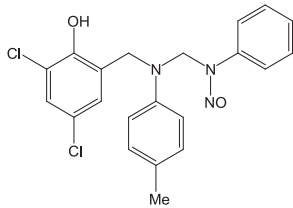
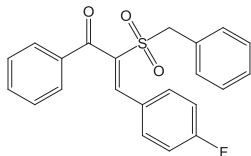
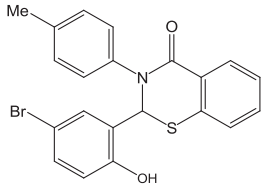
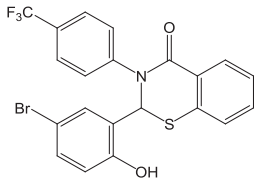
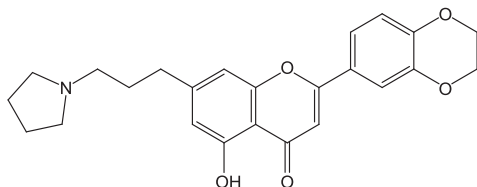
2. Results and discussion

2.1. Virtual screening

In this procedure, the docking program AutoDock 4.0 was used as the *in silico* screening tool [24,25]. The BRAF^{V600E}/SB-590885

crystal structure with the inhibitor removed from the coordinates (PDB ID: 2FB8) [23] was used as a receptor for compound binding. Residues within a distance of 6 Å around the BRAF inhibitor SB-590885 were isolated for the construction of a grid for docking simulation. This grid was large enough to include every residue of the BRAF kinase ATP-binding pocket [26]. The binding affinity of candidate compounds was evaluated by the binding free energies (ΔG_b , kcal/mol, Binding Energy = Intermolecular Energy + Internal Energy + Torsional Energy - Unbound Extended Energy). The compounds which revealed the highest binding affinities were owned lowest predicted binding free energies. After screening from our compound collection, on the basis of their binding affinities with the ATP-binding pocket of BRAF, five initially hits were selected for protein kinase inhibitory activity screening. Their structure, predicted binding free energies and IC₅₀ BRAF^{V600E} were summarized in Table 1; the results indicated that (E)- α -benzylsulfonyl chalcone derivative **Hit 2** exhibited optimal activity with IC₅₀ value of 1.04 μ M. However, the N-nitrosoureas derivative **Hit 1**, thiazolidinyl derivatives **Hit 3** and **Hit 4**, and luteolin derivative **Hit 5**, those compounds owned *in silico* calculated binding free energies comparable to **Hit 2**, did not shown favorable protein kinase inhibitory activities. To obtain more direct insight into the binding

Table 1
Initially virtual screening and protein kinase inhibitory activities screening results.

Compound	Structure	Binding free energies ΔG_b , kcal/mol	BRAF ^{V600E} IC ₅₀ , μ M
Hit 1		−21.87	8.61, 10.92 ^b
Hit 2		−21.75	1.04 ^a
Hit 3		−21.36	>25 ^b
Hit 4		−21.02	>25 ^b
Hit 5		−19.49	10.63, 14.77 ^b

^a Result values are shown as mean values of three independent determinations.

^b Result values are shown as mean values of two independent determinations.

mode of **Hit 2** to mutant BRAF, the binding model of **Hit 2** docked into the active site of BRAF is shown in Fig. 1, which was stimulated by using AutoDock 4.0. Visual inspection of the pose of **Hit 2** into BRAF binding site revealed that this candidate BRAF inhibitor was tightly embedded into the ATP-binding pocket. As shown in Fig. 1b, the model suggests that extensive hydrophobic interactions are formed between **Hit 2** and residues Val 471, Ala 481, Lys 483, Glu 501, Leu 514, Ile 527, Thr 529, Trp 531, Cys 532, Phe 583 and Asp 594 of the ATP-binding pocket of BRAF kinase. Furthermore, in addition to π – π stacking interactions with Trp 531 and Phe 583, which were established by aromatic ring A and C of (E)- α -benzylsulfonyl chalcone skeleton, cation– π interaction was also found between the face of an electron-rich π system of aromatic ring B and Lys 483.

2.2. Chemistry

On the basis of the positive results obtained with (E)- α -benzylsulfonyl chalcone derivative **Hit 2**, the (E)- α -benzylsulfonyl chalcone skeleton could serve as a promising scaffold for developing new kinase inhibitors of V600E mutant BRAF. A serial of novel (E)- α -benzylsulfonyl chalcones prepared as described elsewhere with some modifications [27], the general pathway outlined in Scheme 1. Several substitution were introduced into the A ring and B ring of sulfonyl chalcone skeleton and then 28 (E)- α -benzylsulfonyl chalcones were synthesized in four steps. For the synthesis of compounds **13–40**, phenacyl bromides **1–4** were synthesized from acetophenones and then reacted with benzyl mercaptan to produce phenacyl benzylsulfides **5–8**. Oxidation of phenacyl benzylsulfides **5–8** with 30% hydrogen peroxide in the presence of glacial acetic acid gave phenacyl benzylsulfonyl compounds **9–12**. Knoevenagel condensation of **9–12** with benzaldehyde in glacial acetic acid in the presence of ammonium

Table 2
BRAF^{V600E} kinase and cellular activity of (E)- α -Benzylsulfonyl chalcone analogs **13–40**.

Compound	R ₁	R ₂	IC ₅₀ BRAF ^{V600E} (μ M) ^a	GI ₅₀ WM266.4 (μ M) ^a
13 (Hit 2)	H	4-F	1.04	1.07
14	H	4-NO ₂	0.73	0.54
15	H	4-Br	1.93	1.41
16	H	4-Cl	1.47	1.58
17	H	4-CF ₃	2.44	3.44
18	H	2-Cl	7.3	6.54
19	H	2-NO ₂	3.6	6.7
20	4-Br	2-NO ₂	3.58	4.37
21	4-Br	4-Cl	1.06	0.71
22	4-Br	4-Br	2.01	1.26
23	4-Br	4-CF ₃	3.67	4.27
24	4-Br	4-F	0.79	0.6
25	4-Br	4-NO ₂	0.57	0.51
26	4-Br	2-Cl	4.18	3.44
27	4-OMe	4-Br	2.42	3.58
28	4-OMe	4-NO ₂	1.57	2.03
29	4-OMe	4-Cl	1.92	3.89
30	4-OMe	4-CF ₃	2.94	3.36
31	4-OMe	2-NO ₂	5.95	4.70
32	4-OMe	4-F	1.86	2.06
33	4-OMe	2-Cl	6.6	5.84
34	4-Cl	4-CF ₃	3.01	1.95
35	4-Cl	4-Cl	0.63	0.79
36	4-Cl	2-NO ₂	1.44	1.84
37	4-Cl	4-Br	1.7	1.32
38	4-Cl	4-NO ₂	0.17	0.52
39	4-Cl	4-F	0.29	0.67
40	4-Cl	2-Cl	3.79	4.75
Sorafenib ^b			0.06	8.3

^a Result values are presented from at least three separated experiments.

^b Used as a positive control.

acetate yielded (E)- α -benzylsulfonyl chalcones **13–40**. All the (E)- α -benzylsulfonyl chalcone derivatives were synthesized for the first time and all the compounds were fully characterized by ¹H NMR, ESI-MS and elemental analysis.

2.3. Bioassays

The biological activities of the 28 compounds were determined using two assays: (a) the BRAF^{V600E} inhibitory activities of these synthesized compounds were determined as their ability to inhibit BRAF mediated MEK phosphorylation (IC₅₀ BRAF^{V600E}); (b) the determination of the growth inhibition in WM266.4 human melanoma cells expressing V600E mutant BRAF with MTT assay (GI₅₀ WM266.4). The data are summarized in Table 2.

A number of synthesized analogs displayed potent BRAF^{V600E} kinase inhibitory activities comparable to positive control Sorafenib. In general, six compounds (**14**, **24**, **25**, **35**, **38** and **39**) demonstrated IC₅₀ values being less than **Hit 2**. Compound **38** exhibited the most potential inhibitory activity in tumor growth inhibition (IC₅₀ = 0.17 μ M). Compounds those contain electronic-withdrawing halogen substituents (Cl or Br) on phenyl ring A showed slightly more potent inhibitory activities but did not improved significantly. Compounds bearing the same substituents

Table 3
BRAF^{WT} cellular activity and BRAF^{V600E} cell based pERK activity of selected compounds.

Compound	14 ^a	38	39
GI ₅₀ WM1361 (μ M)	4.24, 5.16	3.56	3.1
IC ₅₀ pERK (μ M)	1.37, 1.63	1.23	1.78

^a Result values are presented from two separated experiments. Others were presented from three separated experiments.

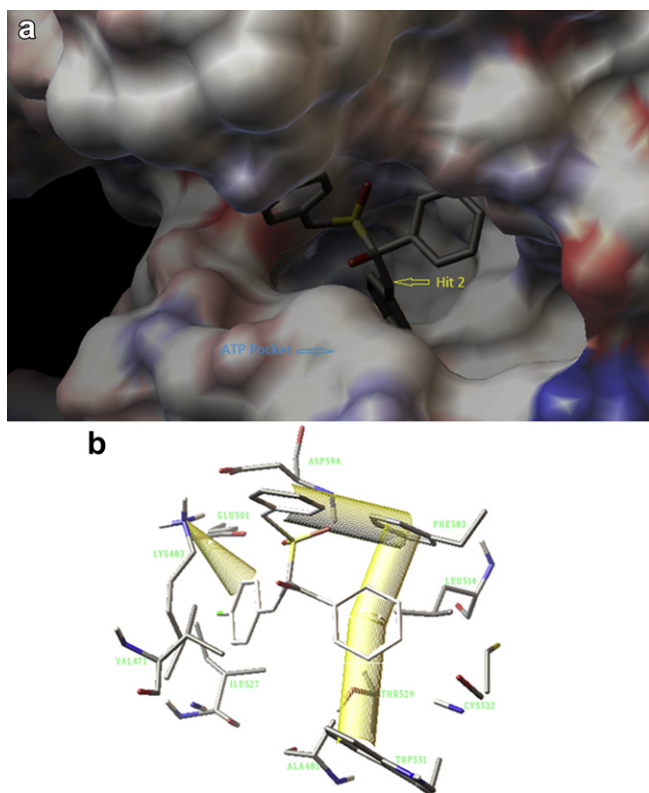
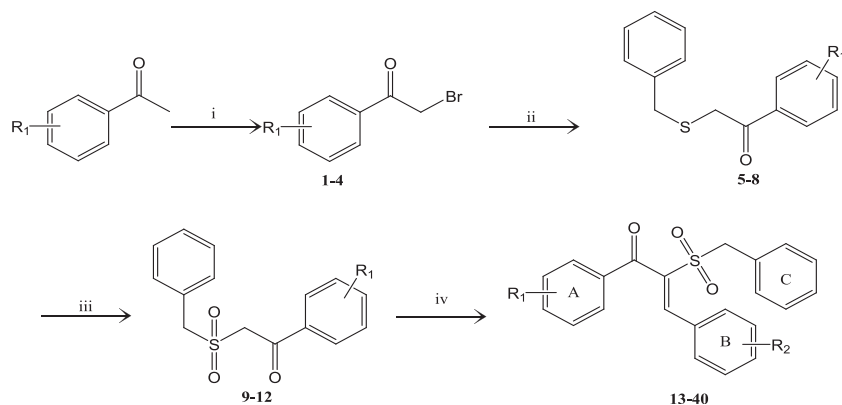


Fig. 1. **Hit 2** bound into ATP pocket of BRAF. Both side chains of important active site amino acids and interaction between ligand and receptor are shown.



Scheme 1. Synthesis route of (E)- α -benzylsulfonyl chalcone derivatives **13–40**. R_1 = 4-Br, 4-Cl, 4-Br and 4-OMe; R_2 = 4-F, 4-NO₂, 4-Br, 4-Cl, 4-CF₃, 2-NO₂ and 2-Cl. Reagents and conditions: (i) bromine, methanol, 0 °C, 5–6 h; (ii) benzyl mercaptan, sodium hydroxide, methanol, rt, 2 h; (iii) 30% hydrogen peroxide, acetic acid, 70 °C, 2 h; (iiii) benzaldehyde, ammonium acetate, acetic acid, reflux, overnight.

on phenyl ring A exhibited distinct kinase inhibitory activity due to the difference of the substituents on the ring B. The inhibitory activity of compounds with different substituents on ring B increased in the following order: 2-Cl < 2-NO₂ < 4-CF₃ < 4-Br < 4-Cl < 4-F < 4-NO₂. This result indicated that the strongly *para* electronic-withdrawing substituents on phenyl ring B were beneficial for the activity. It is worth mentioning that, compounds **14**, **25**, **28** and **38** which with *para*-nitro substituents on phenyl ring B of benzylsulfonyl chalcone skeleton exhibited better potent BRAF^{V600E} inhibitory activity, which suggested that *para*-nitro substituents on ring B was beneficial for kinase inhibitory activities to BRAF. These results clearly showed that the modification of the phenyl ring B can greatly enhance the activity of the compounds.

As described above, the V600E mutant BRAF protein kinase was considered as an important target for the development of small molecule inhibitors in the treatment of human cancers, particularly melanoma. The synthesized (E)- α -benzylsulfonyl chalcone derivatives **13–40** were evaluated for antiproliferative activities against WM266.4 human melanoma cell line expressing V600E mutant BRAF. As illustrated in Table 2, all the compounds displayed IC₅₀ ranging from 0.51 to 6.7 μ M. We observed that these compounds, which have potent BRAF^{V600E} kinase inhibitory activities, displayed corresponding optimal cytotoxic activities against mutant BRAF-dependent WM266.4 cells. These results indicated that these compounds were potential anti-melanoma agents by inhibiting BRAF enzyme, and further validated that V600E mutant BRAF was an effective target of melanoma therapy.

In order to provide evidence for the specificity of the compounds for mutant BRAF-driven cell proliferation, the antiproliferative activities for the BRAF wild-type WM1361 melanoma cell line (GI₅₀ WM1361) that did not express mutant BRAF was determined for selected compounds (**14**, **38** and **39**) and these results were exhibited in Table 3. Compared to the GI₅₀ values on mutant BRAF melanoma cell line WM266.4, the obtained GI₅₀ WM1361 of these inhibitors were all up to dozens of times. Furthermore, for the sake of assess the inhibition of the target signaling pathway (RAF-ERK) by selected compounds, the phosphorylation level of extracellular signal-regulated kinase (ERK) was measured in a cell based assay (IC₅₀ pERK). As shown in Table 3, combined with their GI₅₀ WM266.4, selected compounds exhibited close correlation between the inhibition of both ERK phosphorylation and cell proliferation in a BRAF mutant cell line. These positive results strongly support those designed and synthesized benzylsulfonyl chalcone derivatives possess antiproliferative activities against BRAF melanoma cell line through the selective inhibition of oncogenic BRAF.

In order to evaluate the toxic nature of compound **38**, acute oral toxicity test was introduced. The tested animals appeared normal immediately after administration and did not exhibit any indication of acute toxicity for 14 days afterward. The body weights in treated mice were similar to that of the control mice dosed with an equal volume of vehicle. The result indicated that compound **38** was nontoxic.

3. Conclusion

Virtual screening of our compound collection resulted in the identification of (E)- α -benzylsulfonyl chalcone derivative **Hit 2**, which served as starting point for the design of new V600E mutant BRAF inhibitors. Then a series of novel analogs of hits have been designed and prepared based on the structure of hit compound. Some of the synthesized compounds displayed potent BRAF^{V600E} inhibitory activities. Compound **38** displayed the most potent inhibitory activity, with IC₅₀ value of 0.17 μ M for BRAF^{V600E} and GI₅₀ value of 0.52 μ M for mutant BRAF-dependent WM266.4 cells, comparable to the positive control Sorafenib. Selected compounds which exhibited good inhibitory activities were evaluated their BRAF^{WT} cellular activity and BRAF^{V600E} cell based pERK activity, the results suggested those compounds could selectively inhibit proliferation of mutant BRAF-dependent melanoma cell line through inhibition of oncogenic BRAF. Above all, the results obtained from this study suggest that benzylsulfonyl chalcone skeleton may serve as a novel scaffold for the further development of more potent and selective BRAF^{V600E} inhibitors which use as mutant BRAF-dependent melanoma therapeutic agents.

4. Materials and methods

4.1. Chemistry

4.1.1. Chemistry general

All chemicals (reagent grade) used were purchased from Aldrich (USA). Separation of the compounds by column chromatography was carried out with silica gel 60 (200–300 mesh ASTM, E. Merck, Germany). The quantity of silica gel used was 50–100 times the weight charged on the column. Thin layer chromatography (TLC) was run on the silica gel coated aluminum sheets (silica gel 60 GF254, E. Merck, Germany) and visualized in ultraviolet (UV) light (254 nm). Melting points (uncorrected) were determined with an XT4 MP apparatus (Taikang Corp. Beijing, China). ¹H and ¹³C NMR spectra (300 MHz) were recorded on a ¹H-Varian-Mercury-300 spectrometer at 25 °C, using tetramethylsilane (TMS) as the

internal standard. ESI-MS were recorded with a Mariner System 5304 mass spectrometer. Elementary analyses were performed on a CHN-O-Rapid instrument within $\pm 0.4\%$ of the theoretical values.

4.1.2. Synthesis of 2-benzylthio-1-phenylethanone (**5–8**)

Bromine (3 mL, 60 mmol) was slowly added to a stirred solution of acetophenone (60 mmol) in methanol (40 mL) and temperature of the reaction mixture maintained below 20 °C. After addition of bromine, the contents were stirred at ice bath for further 1–2 h. Then the contents were poured on to ice-water and the solid obtained was collected by filtration. The crude product was recrystallized from ethanol to afford pure α -bromo phenylethanone (**1–4**).

To a solution of sodium hydroxide (30 mmol) in methanol (60 mL) benzyl mercaptan (30 mmol) was added and the contents were stirred at room temperature for 10 min. To this reaction mixture 20 mmol α -Bromo phenylethanone (**1–4**) was added and stirred for further 1–2 h. After completion of the reaction, the contents were cooled, poured on to ice-water and the solid obtained was collected by filtration. The crude product was recrystallized from isopropanol to get pure 2-benzylthio-1-phenylethanone (**5–8**).

4.1.3. Synthesis of 2-benzylsulfonyl-1-phenylethanone (**9–12**)

To a mixture of **5–8** (30 mmol) in glacial acetic acid (60 mL), 30% hydrogen peroxide (36 mL) was added and the contents were refluxed for 1 h. After completion of the reaction, the cooled reaction contents were poured on to ice-water and the separated solid was filtered and dried. The crude product was recrystallized from methanol to obtain pure sample of **9–12**.

4.1.4. General procedure for the preparation of (E)- α -benzylsulfonyl chalcones (**13–40**)

A mixture of 2-Benzylsulfonyl-1-phenylethanone (**9–12**) (1 mmol), benzaldehyde (1 mmol) and ammonium acetate (2.5 mmol) in glacial acetic acid (5 mL) was refluxed overnight. After completion of the reaction, the mixture was evaporated under reduced pressure to give a residue. The residue was purified by silica gel chromatography (PE/EtOAc = 10:1) and recrystallized from isopropanol to afford pure compounds **13–40**.

4.1.4.1. (E)-2-(Benzylsulfonyl)-3-(4-fluorophenyl)-1-phenylprop-2-en-1-one (13**, Hit 2).** Crystal, yield: 76%. m.p. 129–131 °C ^1H NMR (300 MHz, CDCl_3 , δ ppm): 4.61 (s, 2H); 6.83–6.89 (m, 2H); 7.10–7.15 (m, 2H); 7.29–7.41 (m, 6H); 7.51–7.57 (m, 3H); 7.91–7.94 (m, 2H). MS (ESI): 381.1 ($[\text{M} + \text{H}]^+$). Anal. Calcd for $\text{C}_{22}\text{H}_{17}\text{FO}_3\text{S}$: C, 69.46; H, 4.50. Found: C, 69.23; H, 4.16.

4.1.4.2. (E)-2-(Benzylsulfonyl)-3-(4-nitrophenyl)-1-phenylprop-2-en-1-one (14**).** Yellow powder, yield: 81%. m.p. 154–157 °C ^1H NMR (300 MHz, CDCl_3 , δ ppm): 4.63 (s, 2H); 7.29–7.42 (m, 8H); 7.54–7.56 (m, 3H); 7.89–7.92 (m, 2H); 8.01–8.03 (m, 2H). MS (ESI): 408.1 ($[\text{M} + \text{H}]^+$). Anal. Calcd for $\text{C}_{22}\text{H}_{17}\text{NO}_5\text{S}$: C, 64.85; H, 4.21; N, 3.44. Found: C, 64.59; H, 4.00; N, 3.68.

4.1.4.3. (E)-2-(Benzylsulfonyl)-3-(4-bromophenyl)-1-phenylprop-2-en-1-one (15**).** Yellow powder, yield: 70%. m.p. 138–140 °C ^1H NMR (300 MHz, CDCl_3 , δ ppm): 4.60 (s, 2H); 6.97–7.00 (m, 2H); 7.24–7.42 (m, 8H); 7.51–7.58 (m, 3H); 7.91–7.93 (m, 2H). MS (ESI): 441.0 ($[\text{M} + \text{H}]^+$). Anal. Calcd for $\text{C}_{22}\text{H}_{17}\text{BrO}_3\text{S}$: C, 59.87; H, 3.88. Found: C, 59.63; H, 3.98.

4.1.4.4. (E)-2-(Benzylsulfonyl)-3-(4-chlorophenyl)-1-phenylprop-2-en-1-one (16**).** Yellow solid, yield: 70%. m.p. 126–128 °C ^1H NMR (300 MHz, CDCl_3 , δ ppm): 4.63 (s, 2H); 7.29–7.42 (m, 8H); 7.54–7.56

(m, 3H); 7.89–7.91 (m, 2H); 8.03 (d, $J = 8.79$ Hz, 2H). MS (ESI): 381.1 ($[\text{M} + \text{H}]^+$). Anal. Calcd for $\text{C}_{22}\text{H}_{17}\text{FO}_3\text{S}$: C, 69.46; H, 4.50. Found: C, 69.23; H, 4.16.

4.1.4.5. (E)-2-(Benzylsulfonyl)-1-phenyl-3-(4-(trifluoromethyl)phenyl)prop-2-en-1-one (17**).** Yellow solid, yield: 77%. m.p. 92–95 °C ^1H NMR (300 MHz, CDCl_3 , δ ppm): 4.62 (s, 2H); 7.21–7.57 (m, 11H); 7.75 (d, $J = 8.04$ Hz, 2H); 7.90–7.93 (m, 2H); 8.21 (d, $J = 8.04$ Hz, 2H). MS (ESI): 431.1 ($[\text{M} + \text{H}]^+$). Anal. Calcd for $\text{C}_{23}\text{H}_{17}\text{F}_3\text{O}_3\text{S}$: C, 64.18; H, 3.98. Found: C, 63.94; H, 4.13.

4.1.4.6. (E)-2-(Benzylsulfonyl)-3-(2-chlorophenyl)-1-phenylprop-2-en-1-one (18**).** Crystal, yield: 82%. m.p. 130 °C ^1H NMR (300 MHz, CDCl_3 , δ ppm): 4.69 (s, 2H); 6.95–6.99 (m, 2H); 7.09–7.15 (m, 1H); 7.23–7.35 (m, 6H); 7.43–7.48 (m, 1H); 7.56–7.59 (m, 2H); 7.73 (s, 1H); 7.80–7.83 (m, 2H). MS (ESI): 397.0 ($[\text{M} + \text{H}]^+$). Anal. Calcd for $\text{C}_{22}\text{H}_{17}\text{ClO}_3\text{S}$: C, 66.58; H, 4.32. Found: C, 66.81; H, 4.58.

4.1.4.7. (E)-2-(Benzylsulfonyl)-3-(2-nitrophenyl)-1-phenylprop-2-en-1-one (19**).** White solid, yield: 73%. m.p. 173–176 °C ^1H NMR (300 MHz, CDCl_3 , δ ppm): 4.69 (s, 2H); 6.96–7.21 (m, 5H); 7.23–7.59 (m, 7H); 7.71–7.96 (m, 3H). MS (ESI): 408.1 ($[\text{M} + \text{H}]^+$). Anal. Calcd for $\text{C}_{22}\text{H}_{17}\text{NO}_5\text{S}$: C, 64.85; H, 4.21; N, 3.44. Found: C, 65.07; H, 4.03; N, 3.58.

4.1.4.8. (E)-2-(4-Bromobenzylsulfonyl)-3-(2-nitrophenyl)-1-phenylprop-2-en-1-one (20**).** White solid, yield: 90%. m.p. 181–184 °C ^1H NMR (300 MHz, CDCl_3 , δ ppm): 4.69 (s, 2H); 6.96–6.99 (m, 1H); 7.30–7.45 (m, 7H); 7.59–7.67 (m, 4H); 7.83 (s, 1H); 8.01–8.04 (m, 1H). ^{13}C NMR (300 MHz, CDCl_3 , δ ppm): 61.3, 125.2, 128.1, 128.2, 128.7, 129.1, 130.3, 130.7, 131.1, 131.2, 132.1, 133.9, 134.6, 137.3, 143.4, 146.6, 191.2. MS (ESI): 485.9 ($[\text{M} + \text{H}]^+$). Anal. Calcd for $\text{C}_{22}\text{H}_{16}\text{BrNO}_5\text{S}$: C, 54.33; H, 3.32; N, 2.88. Found: C, 54.57; H, 3.14; N, 2.99.

4.1.4.9. (E)-2-(4-Bromobenzylsulfonyl)-3-(4-chlorophenyl)-1-phenylprop-2-en-1-one (21**).** White solid, yield: 72%. m.p. 113–115 °C ^1H NMR (300 MHz, CDCl_3 , δ ppm): 4.63 (s, 2H); 7.03–7.06 (m, 2H); 7.17–7.19 (m, 2H); 7.30–7.33 (m, 4H); 7.50–7.55 (m, 4H); 7.76–7.79 (m, 2H). ^{13}C NMR (300 MHz, CDCl_3 , δ ppm): 61.1, 128.1, 128.6, 128.9, 129.0, 129.6, 129.8, 131.1, 131.2, 134.8, 135.2, 135.6, 137.3, 143.1, 193.2. MS (ESI): 475.0 ($[\text{M} + \text{H}]^+$). Anal. Calcd for $\text{C}_{22}\text{H}_{16}\text{BrClO}_3\text{S}$: C, 55.54; H, 3.39. Found: C, 55.26; H, 3.33.

4.1.4.10. (E)-2-(4-Bromobenzylsulfonyl)-3-(4-bromophenyl)-1-phenylprop-2-en-1-one (22**).** White solid, yield: 75%. m.p. 107–110 °C ^1H NMR (300 MHz, CDCl_3 , δ ppm): 4.63 (s, 2H); 6.97 (d, $J = 8.61$ Hz, 2H); 7.24–7.36 (m, 8H); 7.50–7.55 (m, 4H); 7.77 (d, $J = 8.58$ Hz, 2H). MS (ESI): 518.9 ($[\text{M} + \text{H}]^+$). Anal. Calcd for $\text{C}_{22}\text{H}_{16}\text{Br}_2\text{O}_3\text{S}$: C, 50.79; H, 3.10. Found: C, 50.98; H, 2.92.

4.1.4.11. (E)-2-(4-Bromobenzylsulfonyl)-1-phenyl-3-(4-(trifluoromethyl)phenyl)prop-2-en-1-one (23**).** Yellow solid, yield: 53%. m.p. 113–115 °C ^1H NMR (300 MHz, CDCl_3 , δ ppm): 4.62 (s, 2H); 7.02–7.31 (m, 8H); 7.51–7.78 (m, 4H); 7.97–8.03 (m, 2H). MS (ESI): 509.0 ($[\text{M} + \text{H}]^+$). Anal. Calcd for $\text{C}_{23}\text{H}_{16}\text{BrF}_3\text{O}_3\text{S}$: C, 54.24; H, 3.17. Found: C, 54.51; H, 3.36.

4.1.4.12. (E)-2-(4-Bromobenzylsulfonyl)-3-(4-fluorophenyl)-1-phenylprop-2-en-1-one (24**).** White solid, yield: 69%. m.p. 129–131 °C ^1H NMR (300 MHz, CDCl_3 , δ ppm): 4.61 (s, 2H); 6.89–7.13 (m, 4H); 7.25–7.53 (m, 6H); 7.81–8.04 (m, 4H). MS (ESI): 459.9 ($[\text{M} + \text{H}]^+$). Anal. Calcd for $\text{C}_{22}\text{H}_{16}\text{BrFO}_3\text{S}$: C, 57.53; H, 3.51. Found: C, 57.41; H, 3.60.

4.1.4.13. (*E*)-2-(4-Bromobenzylsulfonyl)-3-(4-nitrophenyl)-1-phenylprop-2-en-1-one (**25**). Yellow solid, yield: 66%. m.p. 145–147 °C ^1H NMR (300 MHz, CDCl_3 , δ ppm): 4.63 (s, 2H); 7.05–7.21 (m, 4H); 7.29–7.59 (m, 7H); 7.62–7.91 (m, 3H). MS (ESI): 485.1 ($[\text{M} + \text{H}]^+$). Anal. Calcd for $\text{C}_{22}\text{H}_{16}\text{BrNO}_5\text{S}$: C, 54.33; H, 3.32; N, 2.88. Found: C, 54.09; H, 3.27; N, 3.03.

4.1.4.14. (*E*)-2-(4-Bromobenzylsulfonyl)-3-(2-chlorophenyl)-1-phenylprop-2-en-1-one (**26**). White solid, yield: 58%. m.p. 131–133 °C ^1H NMR (300 MHz, CDCl_3 , δ ppm): 4.60 (s, 2H); 6.85–6.91 (m, 2H); 7.03–7.11 (m, 2H); 7.21–7.73 (m, 10H). MS (ESI): 474.8 ($[\text{M} + \text{H}]^+$). Anal. Calcd for $\text{C}_{22}\text{H}_{16}\text{BrClO}_3\text{S}$: C, 55.54; H, 3.39. Found: C, 55.43; H, 3.21.

4.1.4.15. (*E*)-3-(4-Bromophenyl)-2-(4-methoxybenzylsulfonyl)-1-phenylprop-2-en-1-one (**27**). White solid, yield: 65%. m.p. 127–129 °C ^1H NMR (300 MHz, CDCl_3 , δ ppm): 3.85 (s, 3H); 4.63 (s, 2H); 6.97–7.02 (m, 2H); 7.12–7.21 (m, 5H); 7.23–7.45 (m, 3H); 7.59–7.71 (m, 4H). MS (ESI): 471.1 ($[\text{M} + \text{H}]^+$). Anal. Calcd for $\text{C}_{23}\text{H}_{19}\text{BrO}_4\text{S}$: C, 58.61; H, 4.06. Found: C, 58.46; H, 4.21.

4.1.4.16. (*E*)-2-(4-Methoxybenzylsulfonyl)-3-(4-nitrophenyl)-1-phenylprop-2-en-1-one (**28**). Yellow solid, yield: 78%. m.p. 163–165 °C ^1H NMR (300 MHz, CDCl_3 , δ ppm): 3.85 (s, 3H); 4.61 (s, 2H); 7.11–7.15 (m, 2H); 7.27–7.36 (m, 6H); 7.57–7.59 (m, 4H); 7.91–8.03 (m, 2H). MS (ESI): 438.1 ($[\text{M} + \text{H}]^+$). Anal. Calcd for $\text{C}_{23}\text{H}_{19}\text{NO}_6\text{S}$: C, 63.15; H, 4.38; N, 3.20. Found: C, 62.97; H, 4.50; N, 3.12.

4.1.4.17. (*E*)-3-(4-Chlorophenyl)-2-(4-methoxybenzylsulfonyl)-1-phenylprop-2-en-1-one (**29**). White solid, yield: 54%. m.p. 112–113 °C ^1H NMR (300 MHz, CDCl_3 , δ ppm): 3.83 (s, 3H); 4.60 (s, 2H); 7.15–7.77 (m, 12H); 7.91–8.01 (m, 2H). MS (ESI): 427.1 ($[\text{M} + \text{H}]^+$). Anal. Calcd for $\text{C}_{23}\text{H}_{19}\text{ClO}_4\text{S}$: C, 64.71; H, 4.49. Found: C, 64.61; H, 4.26.

4.1.4.18. (*E*)-2-(4-Methoxybenzylsulfonyl)-1-phenyl-3-(4-(trifluoromethyl)phenyl)prop-2-en-1-one (**30**). Yellow solid, yield: 60%. m.p. 107–110 °C ^1H NMR (300 MHz, CDCl_3 , δ ppm): 3.85 (s, 3H); 4.61 (s, 2H); 6.97–7.13 (m, 3H); 7.21–7.61 (m, 7H); 7.79–7.92 (m, 4H). MS (ESI): 461.1 ($[\text{M} + \text{H}]^+$). Anal. Calcd for $\text{C}_{24}\text{H}_{19}\text{F}_3\text{O}_4\text{S}$: C, 62.60; H, 4.16. Found: C, 62.79; H, 4.21.

4.1.4.19. (*E*)-2-(4-Methoxybenzylsulfonyl)-3-(2-nitrophenyl)-1-phenylprop-2-en-1-one (**31**). Yellow solid, yield: 72%. m.p. 147–149 °C ^1H NMR (300 MHz, CDCl_3 , δ ppm): 3.83 (s, 3H); 4.63 (s, 2H); 7.07–7.21 (m, 7H); 7.35–7.42 (m, 4H); 7.71–7.80 (m, 1H); 8.05 (d, $J = 8.5$ Hz, 2H). MS (ESI): 438.1 ($[\text{M} + \text{H}]^+$). Anal. Calcd for $\text{C}_{23}\text{H}_{19}\text{NO}_6\text{S}$: C, 63.15; H, 4.38; N, 3.20. Found: C, 62.94; H, 4.24; N, 3.42.

4.1.4.20. (*E*)-3-(4-Fluorophenyl)-2-(4-methoxybenzylsulfonyl)-1-phenylprop-2-en-1-one (**32**). White solid, yield: 80%. m.p. 119–120 °C ^1H NMR (300 MHz, CDCl_3 , δ ppm): 3.85 (s, 3H); 4.63 (s, 2H); 6.95 (d, $J = 8.6$ Hz, 2H); 7.11–7.59 (m, 10H); 7.97–8.11 (m, 2H). MS (ESI): 411.1 ($[\text{M} + \text{H}]^+$). Anal. Calcd for $\text{C}_{23}\text{H}_{19}\text{FO}_4\text{S}$: C, 67.30; H, 4.67. Found: C, 67.22; H, 4.35.

4.1.4.21. (*E*)-3-(2-Chlorophenyl)-2-(4-methoxybenzylsulfonyl)-1-phenylprop-2-en-1-one (**33**). White solid, yield: 67%. m.p. 130–131 °C ^1H NMR (300 MHz, CDCl_3 , δ ppm): 3.85 (s, 3H); 4.63 (s, 2H); 7.12–7.18 (m, 2H); 7.25–7.91 (m, 12H). MS (ESI): 427.1 ($[\text{M} + \text{H}]^+$). Anal. Calcd for $\text{C}_{23}\text{H}_{19}\text{ClO}_4\text{S}$: C, 64.71; H, 4.49. Found: C, 64.96; H, 4.38.

4.1.4.22. (*E*)-2-(4-Chlorobenzylsulfonyl)-1-phenyl-3-(4-(trifluoromethyl)phenyl)prop-2-en-1-one (**34**). Yellow solid, yield: 52%. m.p. 127–129 °C ^1H NMR (300 MHz, CDCl_3 , δ ppm): 4.60 (s, 2H);

6.89–6.97 (m, 2H); 7.09–7.20 (m, 2H); 7.43–7.79 (m, 7H); 7.81–7.85 (m, 1H); 7.91–7.94 (m, 2H). MS (ESI): 465.1 ($[\text{M} + \text{H}]^+$). Anal. Calcd for $\text{C}_{23}\text{H}_{16}\text{ClF}_3\text{O}_3\text{S}$: C, 59.42; H, 3.47. Found: C, 59.66; H, 3.29.

4.1.4.23. (*E*)-2-(4-Chlorobenzylsulfonyl)-3-(4-chlorophenyl)-1-phenylprop-2-en-1-one (**35**). White solid, yield: 79%. m.p. 137–140 °C ^1H NMR (300 MHz, CDCl_3 , δ ppm): 4.58 (s, 2H); 6.96–6.99 (d, $J = 8.58$ Hz, 2H); 7.24–7.38 (m, 8H); 7.50–7.53 (m, 2H); 7.84–7.87 (d, $J = 8.58$ Hz, 2H). MS (ESI): 431.1 ($[\text{M} + \text{H}]^+$). Anal. Calcd for $\text{C}_{22}\text{H}_{16}\text{Cl}_2\text{O}_3\text{S}$: C, 61.26; H, 3.74. Found: C, 61.13; H, 3.80.

4.1.4.24. (*E*)-2-(4-Chlorobenzylsulfonyl)-3-(2-nitrophenyl)-1-phenylprop-2-en-1-one (**36**). Yellow solid, yield: 65%. m.p. 159–161 °C ^1H NMR (300 MHz, CDCl_3 , δ ppm): 4.61 (s, 2H); 6.97 (d, $J = 8.6$ Hz, 2H); 7.23–7.41 (m, 9H); 7.81–7.86 (m, 3H). MS (ESI): 442.1 ($[\text{M} + \text{H}]^+$). Anal. Calcd for $\text{C}_{22}\text{H}_{16}\text{ClNO}_5\text{S}$: C, 59.80; H, 3.65; N, 3.17. Found: C, 59.64; H, 3.05; N, 3.43.

4.1.4.25. (*E*)-3-(4-Bromophenyl)-2-(4-chlorobenzylsulfonyl)-1-phenylprop-2-en-1-one (**37**). White solid, yield: 56%. m.p. 131–133 °C ^1H NMR (300 MHz, CDCl_3 , δ ppm): 4.63 (s, 2H); 6.83–6.91 (m, 2H); 7.21–7.49 (m, 10H); 7.61–7.65 (m, 2H). MS (ESI): 474.9 ($[\text{M} + \text{H}]^+$). Anal. Calcd for $\text{C}_{22}\text{H}_{16}\text{BrClO}_3\text{S}$: C, 55.54; H, 3.39. Found: C, 55.71; H, 3.45.

4.1.4.26. (*E*)-2-(4-Chlorobenzylsulfonyl)-3-(4-nitrophenyl)-1-phenylprop-2-en-1-one (**38**). Yellow solid, yield: 84%. m.p. 104–107 °C ^1H NMR (300 MHz, CDCl_3 , δ ppm): 4.61 (s, 2H); 6.83–6.89 (m, 2H); 7.10–7.15 (m, 2H); 7.29–7.41 (m, 6H); 7.51–7.60 (m, 2H); 7.91–7.94 (m, 2H). MS (ESI): 442.1 ($[\text{M} + \text{H}]^+$). Anal. Calcd for $\text{C}_{22}\text{H}_{16}\text{ClNO}_5\text{S}$: C, 59.80; H, 3.65. Found: C, 59.67; H, 3.72.

4.1.4.27. (*E*)-2-(4-Chlorobenzylsulfonyl)-3-(4-fluorophenyl)-1-phenylprop-2-en-1-one (**39**). Yellow solid, yield: 42%. m.p. 123–125 °C ^1H NMR (300 MHz, CDCl_3 , δ ppm): 4.59 (s, 2H); 6.99 (d, $J = 8.6$ Hz, 2H); 7.21–7.89 (m, 12H). MS (ESI): 415.1 ($[\text{M} + \text{H}]^+$). Anal. Calcd for $\text{C}_{22}\text{H}_{16}\text{ClFO}_3\text{S}$: C, 63.69; H, 3.89. Found: C, 63.45; H, 4.03.

4.1.4.28. (*E*)-2-(4-Chlorobenzylsulfonyl)-3-(2-chlorophenyl)-1-phenylprop-2-en-1-one (**40**). Yellow solid, yield: 66%. m.p. 139–141 °C ^1H NMR (300 MHz, CDCl_3 , δ ppm): 4.65 (s, 2H); 6.83–6.99 (m, 2H); 6.97–7.21 (m, 4H); 7.32–7.59 (m, 5H); 7.69–7.87 (m, 3H). MS (ESI): 431.1 ($[\text{M} + \text{H}]^+$). Anal. Calcd for $\text{C}_{22}\text{H}_{16}\text{Cl}_2\text{O}_3\text{S}$: C, 61.26; H, 3.74. Found: C, 61.47; H, 3.90.

4.2. Biological assays

4.2.1. Antiproliferative activity

WM266.4 and WM1361 melanoma cells (ATCC) were cultured in DMEM/10% fetal bovine serum, in 5% CO_2 water saturated atmosphere at 37 °C. Cell suspensions (10,000/mL) were prepared and 100 μL /well dispensed into 96-well plates (Costar) giving 1000 cells/well. The plates were returned to the incubator for 24 h to allow the cells to reattach. The compounds were initially prepared at 20 mM in DMSO. Aliquots (200 μL) were diluted into 20 mL culture medium giving 200 μM , and 10 serial dilutions of $3 \times$ prepared. Aliquots (100 μL) of each dilution were added to the wells, giving doses ranging from 100 μM to 0.005 μM . After a further incubated at 37 °C for 24 h in a humidified atmosphere with 5% CO_2 , the cell viability was assessed by the conventional 3-(4,5-dimethylthiazol-2-yl)-2,5-diphenyltetrazolium bromide (MTT) reduction assay and carried out strictly according to the manufacturer instructions (Sigma). The absorbance at 590 nm was recorded using LX300 Epson Diagnostic microplate reader. Then GI_{50} was calculated using SPSS 13.0 software.

4.2.2. Kinase assay

This V600E mutant kinase assay was performed in triplicate for each tested compound in this study. Briefly, 7.5 ng Mouse Full-Length GST-tagged BRAF^{V600E} (Invitrogen, PV3849) was pre-incubated at room temperature for 1 h with 1 μ L drug and 4 μ L assay dilution buffer. The kinase assay was initiated when 5 μ L of a solution containing 200 ng recombinant human full-length, N-terminal His-tagged MEK1 (Invitrogen), 200 μ M ATP (0.8 μ Ci hot ATP), and 30 mM MgCl₂ in assay dilution buffer was added. The kinase reaction was allowed to continue at room temperature for 25 min and was then quenched with 5 μ L 5 \times protein denaturing buffer (LDS) solution. Protein was further denatured by heating for 5 min at 70 °C. 10 μ L of each reaction was loaded into a 15-well, 4–12% precast NuPage gel (Invitrogen) and run at 200 V, and upon completion, the front, which contained excess hot ATP, was cut from the gel and discarded. The gel was then dried and developed onto a phosphor screen. A reaction that contained no active enzyme was used as a negative control, and a reaction without inhibitor was used as the positive control.

Detection of the effect of compounds on cell based pERK1/2 activity in WM266.4 cells was performed using ELISA kits (Invitrogen) and strictly according to the manufacturer instructions.

4.3. Molecular docking

The compound library we used for virtual screening of novel BRAF inhibitors in this study was established by our laboratory. This library was a collection of more than 1130 compounds which we designed or synthesized.

The X-ray crystal structure of the BRAF kinase domain in an active configuration (BRAF^{V600E}/SB-590885, PDB code: 2FB8, Protein Data Bank) was used as the target structure in this approach. We used the active site of the crystal structure with the inhibitor excluded from the coordinates as a receptor for compound binding. Residues around SB-590885 at a radius of 6 Å were isolated for the construction of the grid for docking screening. This radius was large enough to include all of the residues that are involved in inhibitor binding.

Studies were carried out on only one subunit of the enzymes. The graphical user interface Autodocktools(ADT) was employed to setup the enzymes: all hydrogens were added, Gasteiger charges were calculated and nonpolar hydrogens were merged to carbon atoms. For macromolecules, generated pdbqt files were saved. Studies were carried out on only one subunit of the enzymes. The graphical user interface ADT was employed to setup the enzymes: all hydrogens were added, Gasteiger charges were calculated and nonpolar hydrogens were merged to carbon atoms. For macromolecules, generated pdbqt files were saved. AutoDock 4.0 software was introduced as the primary screening tool for docking calculations. Default settings were used with an initial population of 50 randomly placed individuals, a maximum number of 2.5×10^6 energy evaluations, and a maximum number of 2.7×10^4 generations. A mutation rate of 0.02 and a crossover rate of 0.8 were chosen. Results differing by less than 0.5 Å in positional root-meansquare deviation (RMSD) were clustered together and the results of the most favorable free energy of binding were selected as the resultant complex structures. The binding affinity was evaluated by the binding free energies (ΔG_b , kcal/mol). The compounds which exhibited the highest binding affinities, which means lowest binding free energies, were chosen.

4.4. Acute oral toxicity of compound 38

Acute oral toxicity studies were performed according to the method of Vasudevan et al. [28] Briefly, mice of either sex, selected by a random sampling technique, were employed in this study. Mice ($n = 3$) in each group were fasted for 4 h with free access to

water only. Compound 38, suspended with carboxymethyl cellulose, (CMC, 0.5% w/v) was administered orally at doses of 50, 250, or 1000 mg kg⁻¹. Appearance and mortality of test animals were observed for 14 days.

Acknowledgments

This work was supported by Jiangsu National Science Foundation (No. BK2009239) and the Fundamental Research Funds for the Central Universities (No. 1092020804 & 1106020824).

Appendix. Supplementary data

Supplementary data related to this article can be found online at doi:10.1016/j.ejmech.2012.02.007.

References

- [1] M.J. Robinson, M.H. Cobb, Mitogen-activated protein kinase pathways, *Current Opinion in Cell Biology* 9 (1997) 180–186.
- [2] J.M. Kyriakis, J. Avruch, Mammalian mitogen-activated protein kinase signal transduction pathways activated by stress and inflammation, *Physiological Reviews* 81 (2001) 807–869.
- [3] G.L. Johnson, R. Lapadat, Mitogen-activated protein kinase pathways mediated by ERK, JNK, and p38 protein kinases, *Science* 298 (2002) 1911–1912.
- [4] G. Pearson, F. Robinson, T.B. Gibson, B.E. Xu, M. Karandikar, K. Berman, M.H. Cobb, Mitogen-activated protein (MAP) kinase pathways: regulation and physiological functions, *Endocrine Reviews* 22 (2001) 153–183.
- [5] P. Cohen, Protein kinases - the major drug targets of the twenty-first century? *Nature Reviews Drug Discovery* 1 (2002) 309–315.
- [6] C. Wellbrock, M. Karasarides, R. Marais, The RAF proteins take centre stage, *Nature Reviews Molecular Cell Biology* 5 (2004) 875–885.
- [7] S.S. Sridhar, D. Hedley, L.L. Siu, Raf kinase as a target for anticancer therapeutics, *Molecular Cancer Therapeutics* 4 (2005) 677–685.
- [8] J. Avruch, A. Khokhlatchev, J.M. Kyriakis, Z.J. Luo, G. Tzivion, D. Vavvas, X.F. Zhang, Ras activation of the Raf kinase: tyrosine kinase recruitment of the MAP kinase cascade, *Recent Progress in Hormone Research* 56 (2001) 127–155.
- [9] H. Davies, G.R. Bignell, C. Cox, P. Stephens, S. Edkins, S. Clegg, J. Teague, H. Woffendin, M.J. Garnett, W. Bottomley, N. Davis, N. Dicks, R. Ewing, Y. Floyd, K. Gray, S. Hall, R. Hawes, J. Hughes, V. Kosmidou, A. Menzies, C. Mould, A. Parker, C. Stevens, S. Watt, S. Hooper, R. Wilson, H. Jayatilake, B.A. Gusterson, C. Cooper, J. Shipley, D. Hargrave, K. Pritchard-Jones, N. Maitland, G. Chenevix-Trench, G.J. Riggins, D.D. Bigner, G. Palmieri, A. Cossu, A. Flanagan, A. Nicholson, J.W.C. Ho, S.Y. Leung, S.T. Yuen, B.L. Weber, H.F. Siegler, T.L. Darrow, H. Paterson, R. Marais, C.J. Marshall, R. Wooster, M.R. Stratton, P.A. Futreal, Mutations of the BRAF gene in human cancer, *Nature* 417 (2002) 949–954.
- [10] J.H. Lee, E.S. Lee, Y.S. Kim, Clinicopathologic significance of BRAF V600E mutation in papillary carcinomas of the thyroid - a meta-analysis, *Cancer* 110 (2007) 38–46.
- [11] M.J. Garnett, R. Marais, Guilty as charged: B-RAF is a human oncogene, *Cancer Cell* 6 (2004) 313–319.
- [12] P.T.C. Wan, M.J. Garnett, S.M. Roe, S. Lee, D. Niculescu-Duvaz, V.M. Good, C.M. Jones, C.J. Marshall, C.J. Springer, D. Barford, R. Marais, P. Cancer Genome, Mechanism of activation of the RAF-ERK signaling pathway by oncogenic mutations of B-RAF, *Cell* 116 (2004) 855–867.
- [13] C. Wellbrock, L. Ogilvie, D. Hedley, M. Karasarides, J. Martin, D. Niculescu-Duvaz, C.J. Springer, R. Marais, B-V599E-RAF is an oncogene in melanocytes, *Cancer Research* 64 (2004) 2338–2342.
- [14] J.S. Sebolt-Leopold, R. Herrera, Targeting the mitogen-activated protein kinase cascade to treat cancer, *Nature Reviews Cancer* 4 (2004) 937–947.
- [15] V. Gray-Schopfer, C. Wellbrock, R. Marais, Melanoma biology and new targeted therapy, *Nature* 445 (2007) 851–857.
- [16] M. Karasarides, A. Chiloche, R. Hayward, D. Niculescu-Duvaz, I. Scanlon, F. Friedlos, L. Ogilvie, D. Hedley, J. Martin, C.J. Marshall, C.J. Springer, R. Marais, B-RAF is a therapeutic target in melanoma, *Oncogene* 23 (2004) 6292–6298.
- [17] B.B. Friday, A.A. Adjei, Advances in targeting the Ras/Raf/MEK/Erk mitogen-activated protein kinase cascade with MEK inhibitors for cancer therapy, *Clinical Cancer Research* 14 (2008) 342–346.
- [18] A.E. Gould, R. Adams, S. Adhikari, K. Aertgeerts, R. Afroze, C. Blackburn, E.F. Calderwood, R. Chau, J. Chouitar, M.O. Duffey, D.B. England, C. Farrer, N. Forsyth, K. Garcia, J. Gaulin, P.D. Greenspan, R.B. Guo, S.J. Harrison, S.C. Huan, N. Iartchouk, D. Janowick, M.S. Kim, B. Kulkarni, S.P. Langston, J.X. Liu, L.T. Ma, S. Menon, H. Mizutani, E. Paske, C.C. Renou, M. Rezaei, R.S. Rowland, M.D. Sintchak, M.D. Smith, S.G. Stroud, M. Tregay, Y.A. Tian, O.P. Veiby, T.J. Vos, S. Vyskocil, J. Williams, T.L. Xu, J.J. Yang, J. Yano, H.B. Zeng, D.M. Zhang, Q. Zhang, K.M. Galvin, Design and optimization of potent and

- orally bioavailable Tetrahydronaphthalene Raf inhibitors, *Journal of Medicinal Chemistry* 54 (2011) 1836–1846.
- [19] G. Bollag, P. Hirth, J. Tsai, J.Z. Zhang, P.N. Ibrahim, H.N. Cho, W. Spevak, C. Zhang, Y. Zhang, G. Habets, E. Burton, B. Wong, G. Tsang, B.L. West, B. Powell, R. Shellooe, A. Marimuthu, H. Nguyen, K.Y.J. Zhang, D.R. Artis, J. Schlessinger, F. Su, B. Higgins, R. Iyer, K. D'Andrea, A. Koehler, M. Stumm, P.S. Lin, R.J. Lee, J. Grippo, I. Puzanov, K.B. Kim, A. Ribas, G.A. McArthur, J.A. Sosman, P.B. Chapman, K.T. Flaherty, X.W. Xu, K.L. Nathanson, K. Nolop, Clinical efficacy of a RAF inhibitor needs broad target blockade in BRAF-mutant melanoma, *Nature* 467 (2010) 596–599.
- [20] C. Wellbrock, A. Hurlstone, BRAF as therapeutic target in melanoma, *Biochemical Pharmacology* 80 (2010) 561–567.
- [21] K.S.M. Smalley, M. Xiao, J. Villanueva, T.K. Nguyen, K.T. Flaherty, R. Letrero, P. Van Belle, D.E. Elder, Y. Wang, K.L. Nathanson, M. Herlyn, CRAF inhibition induces apoptosis in melanoma cells with non-V600E BRAF mutations, *Oncogene* 28 (2008) 85–94.
- [22] I. Niculescu-Duvaz, E. Roman, S.R. Whittaker, F. Friedlos, R. Kirk, I.J. Scanlon, L.C. Davies, D. Niculescu-Duvaz, R. Marais, C.J. Springer, Novel inhibitors of B-RAF based on a disubstituted pyrazine scaffold. Generation of a nanomolar lead, *Journal of Medicinal Chemistry* 49 (2006) 407–416.
- [23] A.J. King, D.R. Patrick, R.S. Batorsky, M.L. Ho, H.T. Do, S.Y. Zhang, R. Kumar, D.W. Rusnak, A.K. Takle, D.M. Wilson, E. Hugger, L.F. Wang, F. Karreth, J.C. Loughheed, J. Lee, D. Chau, T.J. Stout, E.W. May, C.M. Rominger, M.D. Schaber, L.S. Luo, A.S. Lakdawala, J.L. Adams, R.G. Contractor, K.S.M. Smalley, M. Herlyn, M.M. Morrissey, D.A. Tuveson, P.S. Huang, Demonstration of a genetic therapeutic index for tumors expressing oncogenic BRAF by the kinase inhibitor SB-590885, *Cancer Research* 66 (2006) 11100–11105.
- [24] R. Huey, G.M. Morris, A.J. Olson, D.S. Goodsell, A semiempirical free energy force field with charge-based desolvation, *Journal of Computational Chemistry* 28 (2007) 1145–1152.
- [25] G.M. Morris, R. Huey, W. Lindstrom, M.F. Sanner, R.K. Belew, D.S. Goodsell, A.J. Olson, AutoDock4 and AutoDockTools4: automated docking with selective receptor flexibility, *Journal of Computational Chemistry* 30 (2009) 2785–2791.
- [26] C. Luo, P. Xie, R. Marmorstein, Identification of BRAF inhibitors through in silico screening, *Journal of Medicinal Chemistry* 51 (2008) 6121–6127.
- [27] M.V.R. Reddy, V.R. Pallela, S.C. Cosenza, M.R. Mallireddigari, R. Patti, M. Bonagura, M. Truongcao, B. Akula, S.S. Jatiani, E.P. Reddy, Design, synthesis and evaluation of (E)-alpha-benzylthio chalcones as novel inhibitors of BCR-ABL kinase, *Bioorganic & Medicinal Chemistry* 18 (2010) 2317–2326.
- [28] M. Vasudevan, K.K. Gunnam, M. Parle, Antinociceptive and anti-inflammatory effects of Thespesia populnea bark extract, *Journal of Ethnopharmacology* 109 (2007) 264–270.